1997

Stability Analysis of the Internal Dynamics of a Wheeled Mobile Robot

Yun, Xiaoping; Yamamoto, Yoshio

Journal of Robotic Systems, Volume 14, Issue 10, pp. 697Ã¢ 709 (1997)
http://hdl.handle.net/10945/44185

Stability Analysis of the Internal Dynamics of a Wheeled Mobile Robot

Xiaoping Yun*
Department of Electrical and Computer Engineering
Code EC/Yx
Naval Postgraduate School
Monterey, CA 93943-5121
e-mail: yun@ece.nps.navy.mil

Yoshio Yamamoto
Department of Systems Engineering
Ibaraki University
12-1 Nakanarusawa 4 chome
Hitachi, Ibaraki
316 Japan
e-mail: yoshio@hit.ipc.ibaraki.ac.jp

Received May 15, 1995; accepted May 9, 1997

The stability of the internal dynamics of a wheeled mobile robot is analyzed. It is shown that the wheeled mobile robot exhibits unstable internal dynamics when moving backwards. Most control methods of wheeled mobile robots are designed based on input-output relations. Since the internal dynamics are not represented in input-output relations, stability properties of the internal dynamics are generally neglected. Nevertheless, the internal dynamics do affect the behavior of mobile robots. Taking the look-ahead control method as an example, it is shown that, by using a novel Liapunov function, the internal dynamics of a two-wheel differential-drive mobile robot are unstable when it is commanded to move backwards. Both simulation and experimental results are provided to verify the analysis.

*To whom all correspondence should be addressed.

Journal of Robotic Systems 14(10), 697–709 (1997)

CCC 0741-2223/97/0100697-13

車輪付き移動ロボットの内部力学的安定性について解析する。車輪付き移動ロボットが後退するときに、内部力学的に不安定になることは証明されている。車輪付き移動ロボットのほとんどの制御法は、入出力関係に基づいている。ところが、内部力学は入出力関係では表現できないので、一般的に、内部力学の安定特性は無視される。しかしながら、内部力学は、移動ロボットの動作に悪影響を及ぼす。たとえば、新しいLiapunov関数前方直視制御法では、二輪の差動ドライブ移動ロボットの内部力学が、後退するときに不安定になる。解析結果の検証は、シミュレーションと実験によって行う。

1. INTRODUCTION

Everyone who has learned how to drive an automobile should have noticed that driving backwards is considerably more difficult than driving forwards. Driving backwards over a longer distance and/or at a higher speed is a skill that not everyone possesses. The subject of this article is wheeled mobile robots, not driving, but the driving experience helps explain the problem and results to be presented. The analogy of backward driving versus forward driving in autonomous wheeled mobile robots will be investigated, and it will be shown that ''backward driving'' is inherently unstable.

Feedback control of wheeled mobile robots has recently been studied by many researchers.[1–4] Since dynamics of a wheeled mobile robot are nonlinear, the technique of feedback linearization is commonly used to facilitate the controller design. A wheeled mobile robot is subject to nonholonomic constraints. Because a nonholonomic dynamic system is not input-state linearizable,[5–7] most feedback control methods proposed for wheeled mobile robots use input-output linearization.[1,2,7] Even though the closed-loop input-output map of the mobile robot system using those control methods is linear, the system has nonlinear internal dynamics. While the stability of input-output map is ensured by a proper linear feedback through pole placement, stability properties of the internal dynamics are rarely discussed.

In this article, we study the internal dynamics of a wheeled mobile robot under the look-ahead control. The look-ahead control takes the coordinates of a reference point in front of the mobile robot as the output equation. By using a nonlinear feedback, the input-output map is linearized. A linear feedback is further applied to stabilize the system. With this controller, the reference point can follow any trajectory. Nevertheless, the internal dynamics of this system are not always stable.

By properly choosing a state transformation, the internal dynamics as well as the zero dynamics of the mobile robot are first characterized. The zero dynamics are always stable. The stability of the internal dynamics is then investigated. It turns out that the internal dynamics are unstable under certain conditions. More specifically, using a novel Liapunov function, we show that the internal dynamics are unstable when the mobile robot is commanded to move backwards. Although the unstable behavior of the internal motion has been observed earlier,[8] the analysis of the internal dynamics is presented for the first time. The stable tracking control method presented in reference 9 is established only for the case of moving forwards.

Both a simulation and an experiment have been conducted to verify the theoretical analysis. In the experiment, the look-ahead control method is implemented on a TRC LABMATE mobile platform. It is observed that when the reference point is commanded to move backwards along a straight line, the mobile robot tends to swivel either left or right and to change the heading angle by 180 degrees, depending on minor misalignment of the heading angle or minor variation of floor conditions. The simulation and experimental results are consistent and they confirm that the internal dynamics are unstable when the reference point moves backwards.

2. DYNAMICS OF A WHEELED MOBILE ROBOT

2.1. Constraint Equations

In this section, motion equations and constraint equations of a wheeled mobile robot whose schematic top view is shown in Figure 1 are derived. It is assumed that the mobile robot is driven by two independent wheels and supported by four passive wheels at the

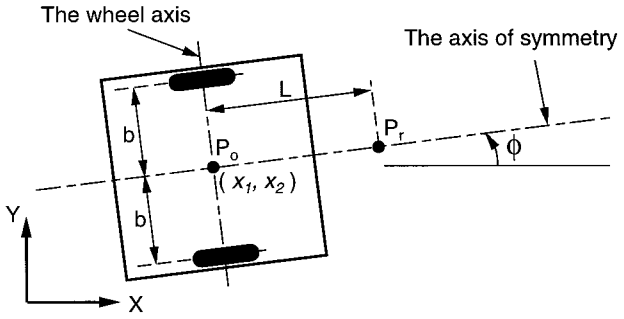

Figure 1. Schematic of the mobile robot.

corners (not shown in Fig. 1). Before proceeding, let us fix some notations (see Fig. 1).

- b: the displacement from each of the driving wheels to the axis of symmetry.
- d: the displacement from point P_o to the mass center of the mobile robot, which is assumed to be on the axis of symmetry.
- r: the radius of the driving wheels.
- c: a constant equal to $r/2b$.
- m_c: the mass of the mobile robot without the driving wheels and the rotors of the motors.
- m_w: the mass of each driving wheel plus the rotor of its motor.
- I_c: the moment of inertia of the mobile robot without the driving wheels and the rotors of the motors about a vertical axis through the intersection of the axis of symmetry with the driving wheel axis.
- I_w: the moment of inertia of each driving wheel and the motor rotor about the wheel axis.
- I_m: the moment of inertia of each driving wheel and the motor rotor about a wheel diameter.

There are three constraints. The first one is that the mobile robot can not move in a lateral direction, i.e.,

$$\dot{x}_2 \cos\phi - \dot{x}_1 \sin\phi = 0 \tag{1}$$

where (x_1, x_2) is the coordinates of point P_o in the fixed reference coordinated frame **X**–**Y**, and ϕ is the heading angle of the mobile robot measured from **X**-axis. The other two constraints are that the two driving wheels roll and do not slip:

$$\dot{x}_1 \cos\phi + \dot{x}_2 \sin\phi + b\dot{\phi} = r\dot{\theta}_1 \tag{2}$$

$$\dot{x}_1 \cos\phi + \dot{x}_2 \sin\phi - b\dot{\phi} = r\dot{\theta}_2 \tag{3}$$

where θ_1 and θ_2 are the angular positions of the two driving wheels, respectively.

By using the techniques of differential geometry, it can be shown that, among the three constraints, two of them are nonholonomic and the third one is holonomic.[7]

To obtain the holonomic constraint, we subtract equation (3) from equation (2).

$$2b\dot{\phi} = r(\dot{\theta}_1 - \dot{\theta}_2) \tag{4}$$

Integrating the above equation and properly choosing the initial condition of ϕ, θ_1, and θ_2, we have

$$\phi = c(\theta_1 - \theta_2) \tag{5}$$

which is clearly a holonomic constraint equation. The two nonholonomic constraints are

$$\dot{x}_1 \sin\phi - \dot{x}_2 \cos\phi = 0 \tag{6}$$

$$\dot{x}_1 \cos\phi + \dot{x}_2 \sin\phi = cb(\dot{\theta}_1 + \dot{\theta}_2) \tag{7}$$

The second nonholonomic constraint equation in the above is obtained by adding equations (2) and (3). These two constraint equations can be written in matrix form

$$A(q)\dot{q} = 0 \tag{8}$$

where

$$q = \begin{bmatrix} q_1 \\ q_2 \\ q_3 \\ q_4 \end{bmatrix} = \begin{bmatrix} x_1 \\ x_2 \\ \theta_1 \\ \theta_2 \end{bmatrix} \tag{9}$$

$$A(q) = \begin{bmatrix} a_{11} & a_{12} & a_{13} & a_{14} \\ a_{21} & a_{22} & a_{23} & a_{24} \end{bmatrix} = \begin{bmatrix} -\sin\phi & \cos\phi & 0 & 0 \\ -\cos\phi & -\sin\phi & cb & cb \end{bmatrix} \tag{10}$$

2.2. Dynamic Equations

We use the Lagrange formulation to establish equations of motion for the mobile robot. The total kinetic energy of the mobile base and the two wheels is

$$K = \frac{1}{2} m(\dot{x}_1^2 + \dot{x}_2^2) + m_c cd(\dot{\theta}_1 - \dot{\theta}_2)(\dot{x}_2 \cos\phi - \dot{x}_1 \sin\phi) + \frac{1}{2} I_w(\dot{\theta}_1^2 + \dot{\theta}_2^2) + \frac{1}{2} Ic^2(\dot{\theta}_1 + \dot{\theta}_2)^2 \tag{11}$$

where

$$m = m_c + 2m_w$$
$$I = I_c + 2m_w b^2 + 2I_m$$

Lagrange equations of motion for the nonholonomic mobile robot system are governed by[10]

$$\frac{d}{dt}\left(\frac{\partial K}{\partial \dot{q}_i}\right) - \frac{\partial K}{\partial q_i} = \tau_i - a_{1i}\lambda_1 - a_{2i}\lambda_2, \quad i = 1, \ldots 4 \tag{12}$$

where q_i is the generalized coordinate defined in equation (9), τ_i is the generalized force, a_{ij}s are the elements of matrix $A(q)$ in equation (10), and λ_1 and λ_2 are the Lagrange multipliers. Substituting the total kinetic energy (Eq. (11)) into Eq. (12), we obtain

$$m\ddot{x}_1 - m_c d(\ddot{\phi}\sin\phi + \dot{\phi}^2\cos\phi) = \lambda_1 \sin\phi + \lambda_2\cos\phi \tag{13}$$

$$m\ddot{x}_2 + m_c d(\ddot{\phi}\cos\phi - \dot{\phi}^2\sin\phi) = -\lambda_1\cos\phi + \lambda_2\sin\phi \tag{14}$$

$$m_c cd(\ddot{x}_2\cos\phi - \ddot{x}_1\sin\phi) + (Ic^2 + I_w)\ddot{\theta}_1 - Ic^2\ddot{\theta}_2 = \tau_1 - cb\lambda_2 \tag{15}$$

$$-m_c cd(\ddot{x}_2\cos\phi - \ddot{x}_1\sin\phi) - Ic^2\ddot{\theta}_1 + (Ic^2 + I_w)\ddot{\theta}_2 = \tau_2 - cb\lambda_2 \tag{16}$$

where τ_1 and τ_2 are the torques acting on the two wheels. These equations can be written in the matrix form

$$M(q)\ddot{q} + V(q,\dot{q}) = E(q)\tau - A^T(q)\lambda \tag{17}$$

where $A(q)$ is defined in equation (10) and

$$M(q) = \begin{bmatrix} m & 0 & -m_c cd\sin\phi & m_c cd\sin\phi \\ 0 & m & m_c cd\cos\phi & -m_c cd\cos\phi \\ -m_c cd\sin\phi & m_c cd\cos\phi & Ic^2 + I_w & -Ic^2 \\ m_c cd\sin\phi & -m_c cd\cos\phi & -Ic^2 & Ic^2 + I_w \end{bmatrix}$$

$$V(q,\dot{q}) = \begin{bmatrix} -m_c d\dot{\phi}^2\cos\phi \\ -m_c d\dot{\phi}^2\sin\phi \\ 0 \\ 0 \end{bmatrix} \qquad E(q) = \begin{bmatrix} 0 & 0 \\ 0 & 0 \\ 1 & 0 \\ 0 & 1 \end{bmatrix}$$

$$\tau = \begin{bmatrix} \tau_1 \\ \tau_2 \end{bmatrix} \qquad \lambda = \begin{bmatrix} \lambda_1 \\ \lambda_2 \end{bmatrix}$$

2.3. State Space Realization

In this subsection, a state space realization of the motion equation (17) and constraint equation (8) is established. Let $S(q)$ be a 4×2 matrix

$$S(q) = [s_1(q)\ s_2(q)] = \begin{bmatrix} cb\cos\phi & cb\cos\phi \\ cb\sin\phi & cb\sin\phi \\ 1 & 0 \\ 0 & 1 \end{bmatrix} \tag{18}$$

whose columns are in the null space of $A(q)$ matrix in the constraint equation (8), i.e., $A(q)S(q) = 0$. From the constraint equation (8), the velocity q must be in the null space of $A(q)$. It follows that $q \in span\{s_1(q), s_2(q)\}$, and that there exists a smooth vector $\eta = [\eta_1\ \eta_2]^T$ such that

$$\dot{q} = S(q)\eta \tag{19}$$

and

$$\ddot{q} = S(q)\dot{\eta} + \dot{S}(q)\eta \tag{20}$$

For the specific choice of $S(q)$ matrix in equation (18), we have $\eta = \dot{\theta}$, where $\dot{\theta} = [\dot{\theta}_1\ \dot{\theta}_2]^T$.

Multiplying both sides of equation (17) by $S^T(q)$ and noticing that $S^T(q)A^T(q) = 0$ and $S^T(q)E(q) = I_{2\times 2}$ (the 2×2 identity matrix), we obtain

$$S^T(q)M(q)\ddot{q} + S^T(q)V(q,\dot{q}) = S^T(q)E(q)\tau = \tau \tag{21}$$

Substituting equation (20) into the above equation, we have

$$S^T(q)M(q)(S(q)\dot{\eta} + \dot{S}(q)\eta) + S^T(q)V(q,\dot{q}) = \tau \tag{22}$$

By choosing the following state variable

$$x = \begin{bmatrix} x_1 \\ x_2 \\ x_3 \\ x_4 \\ x_5 \\ x_6 \end{bmatrix} = \begin{bmatrix} x_1 \\ x_2 \\ \theta_1 \\ \theta_2 \\ \eta_1 \\ \eta_2 \end{bmatrix} = \begin{bmatrix} q \\ \eta \end{bmatrix} \tag{23}$$

the motion equation (22) may be represented in the state space form

$$\dot{x} = f(x) + g(x)\tau \tag{24}$$

where

$$f(x) = \begin{bmatrix} S\dot{\eta} \\ -(S^TMS)^{-1}(S^TMS\dot{\eta} + S^TV) \end{bmatrix},$$

$$g(x) = \begin{bmatrix} 0 \\ (S^TMS)^{-1} \end{bmatrix}$$

Note that the dependent variables for each term have been omitted in the above representation for clarity. All the terms are functions of the state variable x only. Since q is not part of the state variable, it is replaced by $S(q)\eta$ by noting equation (19). To simplify the discussion, the following state feedback is first applied

$$\begin{aligned}\tau &= \alpha^1(x) + \beta^1(x)\mu \\ &= (S^TMS\dot{\eta} + S^TV) + (S^TMS)S^TE\mu\end{aligned} \tag{25}$$

where μ is the new input variable. The closed-loop system becomes

$$\dot{x} = f^1(x) + g^1(x)\mu \tag{26}$$

where

$$f^1(x) = \begin{bmatrix} S\dot{\eta} \\ 0 \end{bmatrix} \qquad g^1(x) = \begin{bmatrix} 0 \\ I_{2\times 2} \end{bmatrix}$$

3. LOOK-AHEAD CONTROL

It is known that the center point P_o of the mobile robot cannot be controlled by using a static feedback, and that an alternative control method is to control a point in front of the mobile robot.[1,2,7] This method is motivated from vehicle maneuvering. When operating a vehicle, a driver looks at a point or an area in front of the vehicle. To facilitate the discussion on the internal dynamics, the look-ahead control method is briefly described. We define a reference point P_r that is a distance L (called look-ahead distance) from P_o (see Fig. 1). The coordinates of P_r in the fixed coordinate frame are taken as the output equation, i.e.,

$$y = h(x) = \begin{bmatrix} x_1 + L\cos\phi \\ x_2 + L\sin\phi \end{bmatrix} \tag{27}$$

To verify if the system is input-output linearizable with this output equation, it is straightforward to compute the derivatives of y.

$$\begin{aligned}\dot{y} &= \frac{\partial h}{\partial x}\dot{x} = \frac{\partial h}{\partial x}(f^1(x) + g^1(x)\mu) \\ &= \begin{bmatrix} cb\cos\phi - cL\sin\phi & cb\cos\phi + cL\sin\phi \\ cb\sin\phi + cL\cos\phi & cb\sin\phi - cL\cos\phi \end{bmatrix}\begin{bmatrix}\eta_1 \\ \eta_2\end{bmatrix} \\ &= \Phi(x)\eta\end{aligned}$$

Since $\dot{y}$ is not a function of the input μ, it is differentiated once more.

$$\ddot{y} = \dot{\Phi}(x)\eta + \Phi(x)\dot{\eta} = \dot{\Phi}(x)\eta + \Phi(x)\mu$$

The input μ shows up in the second order derivative of y. Clearly, the decoupling matrix in this case is $\Phi(x)$. Since the determinant of $\Phi(x)$ is $(-2c^2bL)$, it is nonsingular as long as the look-ahead distance L is not zero. It follows that the system can be input-output linearized and decoupled.[11] The nonlinear feedback for achieving the input-output linearization and decoupling is

$$\mu = \Phi^{-1}(x)(u - \dot{\Phi}(x)\eta) \tag{28}$$

Applying this nonlinear feedback, we obtain

$$\ddot{y}_1 = u_1 \tag{29}$$

$$\ddot{y}_2 = u_2 \tag{30}$$

Therefore, the mobile robot can be controlled so that the reference point P_r tracks a desired trajectory. The motion of the mobile robot itself, particularly the motion of the center point P_o, is determined by the internal dynamics of the system, which are the topic of the next section.

4. INTERNAL DYNAMICS

4.1. Characterizing Internal Dynamics

The previous section introduced the look-ahead control method for the mobile robot. In this section, we

proceed to study the behavior of the internal dynamics, including the zero dynamics of the system. For a general discussion of internal dynamics and zero dynamics, see Chapter 6 of reference 12 or see reference 13.

A diffeomorphism is constructed, by which the overall system can be represented in the normal form of nonlinear systems.[12] Since the relative degree of each output is two, four components of the needed diffeomorphism from the two outputs and its Lie derivative may be constructed, i.e., $h_1(x), L_f h_1(x), h_2(x)$, and $L_f h_2(x)$. Since the state variable x is six dimensional, two more components are needed. θ_1 and θ_2 are chosen to be these two components. Thus the proposed diffeomorphic transformation would be

$$z = T(x) = \begin{bmatrix} z_1 \\ z_2 \\ z_3 \\ z_4 \\ z_5 \\ z_6 \end{bmatrix} = \begin{bmatrix} h_1(x) \\ L_f h_1(x) \\ h_2(x) \\ L_f h_2(x) \\ \theta_1 \\ \theta_2 \end{bmatrix} \tag{31}$$

To verify that $T(x)$ is indeed a diffeomorphism, its Jacobian is computed:

$$\frac{\partial T}{\partial x} = \begin{bmatrix} 1 & 0 & -cL\sin\phi & cL\sin\phi & 0 & 0 \\ 0 & 0 & * & * & cb\cos\phi - cL\sin\phi & cb\cos\phi + cL\sin\phi \\ 0 & 1 & cL\cos\phi & -cL\cos\phi & 0 & 0 \\ 0 & 0 & * & * & cb\sin\phi + cL\cos\phi & cb\sin\phi - cL\cos\phi \\ 0 & 0 & 1 & 0 & 0 & 0 \\ 0 & 0 & 0 & 1 & 0 & 0 \end{bmatrix}$$

It is easy to check that $\partial T/\partial x$ has full rank.[a] Thus $T(x)$ is a valid state space transformation. The inverse information transformation $x = T^{-1}(z)$ is given by

$$\begin{aligned} x_1 &= z_1 - L\cos(cz_5 - cz_6) \\ x_2 &= z_3 - L\sin(cz_5 - cz_0) \\ \theta_1 &= z_5 \\ \theta_2 &= z_6 \\ \begin{bmatrix} \eta_1 \\ \eta_2 \end{bmatrix} &= \Phi^{-1} \begin{bmatrix} z_2 \\ z_4 \end{bmatrix} \end{aligned}$$

We partition the state variable z into two blocks

$$\begin{aligned} z^1 &= [z_1 \quad z_2 \quad z_3 \quad z_4]^T \\ z^2 &= [z_5 \quad z_6]^T \end{aligned}$$

After applying the feedback (28), the system of the mobile robot is represented in the following normal form.

$$\dot{z}^1 = Az^1 + Bu \tag{32}$$

$$\dot{z}^2 = w(z^1, z^2) \tag{33}$$

$$y = Cz^1 \tag{34}$$

where

$$A = \begin{bmatrix} 0 & 1 & 0 & 0 \\ 0 & 0 & 0 & 0 \\ 0 & 0 & 0 & 1 \\ 0 & 0 & 0 & 0 \end{bmatrix}, \qquad B = \begin{bmatrix} 0 & 0 \\ 1 & 0 \\ 0 & 0 \\ 0 & 1 \end{bmatrix},$$

$$C = \begin{bmatrix} 1 & 0 & 0 & 0 \\ 0 & 0 & 1 & 0 \end{bmatrix}$$

$$w(z^1, z^2) = \Phi^{-1}(z) \begin{bmatrix} z_2 \\ z_4 \end{bmatrix} = -\frac{1}{rcL} \begin{bmatrix} cb\sin\phi - cL\cos\phi & -cb\cos\phi - cL\sin\phi \\ -cb\sin\phi - cL\cos\phi & cb\cos\phi - cL\sin\phi \end{bmatrix} \begin{bmatrix} z_2 \\ z_4 \end{bmatrix}$$

It is understood that ϕ in the expression of $w(z^1, z^2)$ is a short-hand notation for $c(z_5 - z_6)$. Together, the linear state equation (32) and the linear output equation (34) are an equivalent representation of the input-output map (Eqs. (29) and (30)). Eq. (33) represents the unobservable internal dynamics of the mobile robot under the look-ahead control.

[a] The terms denoted by $*$ do not affect the computation of the rank.

4.2. Zero Dynamics

The zero dynamics of a control system are defined as the dynamics of the system when the outputs are identically zero (i.e., $y = 0$, $\dot{y} = 0$, $\ddot{y} = 0$, . . .). In this case, $z^1 = 0$, and the zero dynamics are

$$\dot{z}^2 = w(0, z^2) = 0 \tag{35}$$

Thus, z^2 remains constant while the outputs are identically zero. The zero dynamics are stable but not asymptotically stable. In other words, if the reference point P_r remains still, so does the mobile robot (or more specifically, the wheels do not move).

4.3. Stability of Internal Dynamics

We now look at the internal dynamics while the reference point is in motion. More specifically, we are interested in the internal motion of the mobile robot when it moves straight forward or backward. Let the mobile robot be initially headed in the positive **X** direction. It is assumed that the reference point is controlled to move in the negative **X** direction. The position of the reference point is denoted by

$$\begin{bmatrix} y_1 \\ y_2 \end{bmatrix} = \begin{bmatrix} -\varepsilon(t) \\ 0 \end{bmatrix}$$

and the velocity of the reference point is then

$$\begin{bmatrix} \dot{y}_1 \\ \dot{y}_2 \end{bmatrix} = \begin{bmatrix} z_2 \\ z_4 \end{bmatrix} = \begin{bmatrix} -\nu(t) \\ 0 \end{bmatrix}$$

where $\nu(t) = \dot{\varepsilon}(t)$. Since the reference point moves in the negative **X** direction, y_1 is negative and therefore $\nu(t) > 0$. Substituting this into the internal dynamics (33), we obtain

$$\begin{bmatrix} \dot{z}_5 \\ \dot{z}_6 \end{bmatrix} = \frac{\nu(t)}{rcL} \begin{bmatrix} cb \sin\phi - cL\cos\phi \\ -cb \sin\phi - cL\cos\phi \end{bmatrix}$$

A solution of this internal dynamics is

$$z_5^* = -\frac{1}{r}\varepsilon(t) + c_1 \tag{36}$$

$$z_6^* = -\frac{1}{r}\varepsilon(t) + c_1 \tag{37}$$

where c_1 is a constant. That is, the two wheels rotate at exactly the same angular velocity and the mobile platform moves straight in the negative **X** direction.

We now study the stability of the internal motion described by Eqs. (36) and (37). We first change the state variable so that the stability of the internal motion in z^2 can be formulated as the stability of equilibrium points in ζ.

$$\zeta_1 = z_5 - z_5^*$$

$$\zeta_2 = z_6 - z_6^*$$

The internal dynamics may be expressed in terms of $\zeta = [\zeta_1\ \zeta_2]^T$.

$$\dot{\zeta} = \begin{bmatrix} \dot{\zeta}_1 \\ \dot{\zeta}_2 \end{bmatrix} = \frac{\nu(t)}{rcL} \begin{bmatrix} cb\sin(c\zeta_1 - c\zeta_2) - cL\cos(c\zeta_1 - c\zeta_2) \\ -cb\sin(c\zeta_1 - c\zeta_2) - cL\cos(c\zeta_1 - c\zeta_2) \end{bmatrix} + \begin{bmatrix} \frac{1}{r}\nu(t) \\ \frac{1}{r}\nu(t) \end{bmatrix}$$

This system has an equilibrium subspace characterized by

$$E_\zeta = \{\zeta \mid \zeta_1 = \zeta_2\}$$

No conclusion can be drawn based on the linear approximation of the internal dynamics that has an eigenvalue at the origin. The Liapunov method is then used to establish the stability condition. Consider the following candidate for a Liapunov function

$$V(\zeta) = 1 - \cos(c\zeta_1 - c\zeta_2)$$

In a neighborhood of E_ζ, $V(\zeta) = 0$ if $\zeta \in E$, and $V(\zeta) > 0$ if $\zeta \notin E_\zeta$. Thus $V(\zeta)$ is positive definite with respect to E_ζ, and may serve as a Liapunov function for testing the stability of E_ζ. The derivative of $V(\zeta)$ with respect to the time is:

$$\dot{V}(\zeta) = \frac{\partial V}{\partial \zeta}\dot{\zeta} = \sin(c\zeta_1 - c\zeta_2)[c \quad -c]\dot{\zeta}$$

$$= \sin(c\zeta_1 - c\zeta_2)(\dot{\zeta}_1 - \dot{\zeta}_2)c = \frac{\nu(t)}{L}\sin^2(c\zeta_1 - c\zeta_2)$$

Since $\nu(t) > 0$, $\dot{V}(\zeta)$ is also positive definite with respect to E_ζ. Therefore the equilibrium subspace E_ζ is not stable.

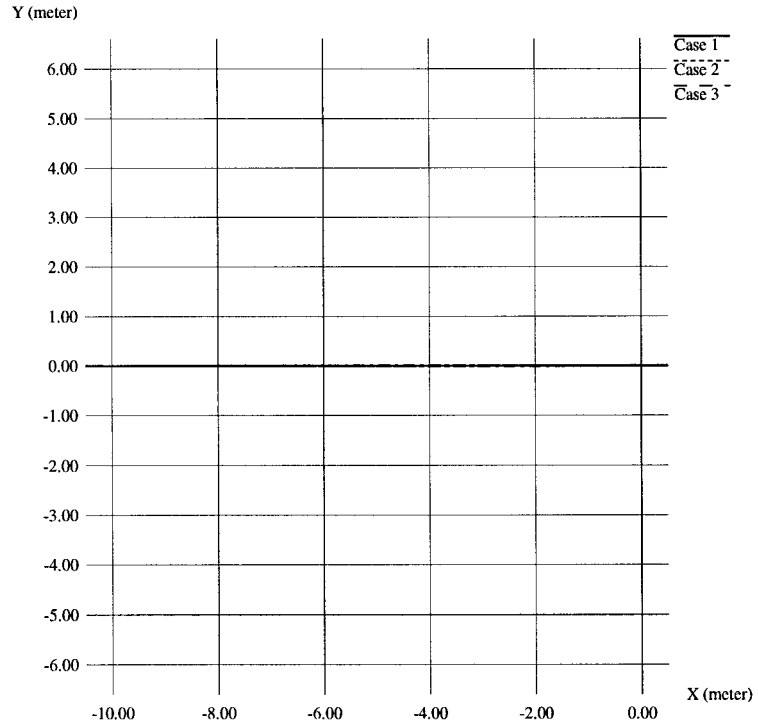

Figure 2. The actual trajectories of the reference point from the simulation. All three curves coincide with the *X*-axis, indicating that the reference point follows the desired trajectory very closely.

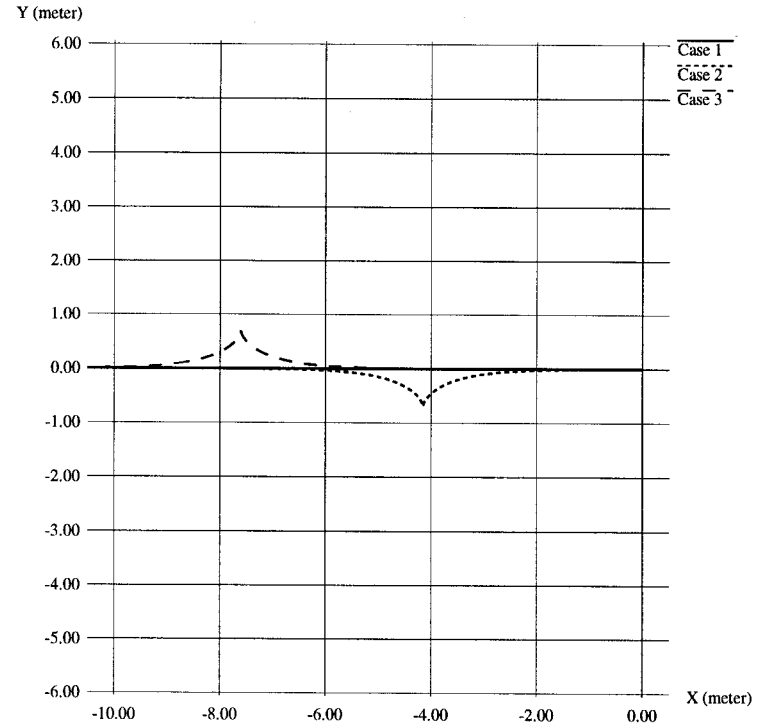

Figure 3. The trajectories of the point P_0 on the wheel axis from the simulation. The curve for the first case coincides with the *X*-axis. The curves for the second and third cases show that the point P_0 departs from the *X*-axis.

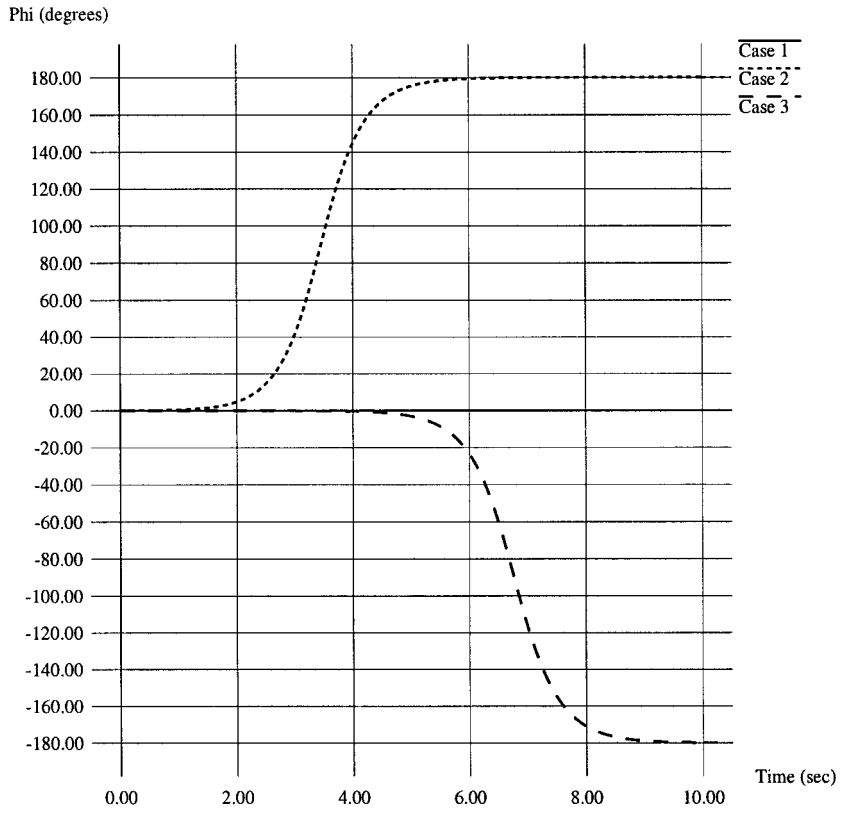

Figure 4. The heading angle of the platform from the simulation. While the heading angle of the first case maintains at zero degrees in the entire duration, the heading angle of the second and third cases changes by 180 degrees.

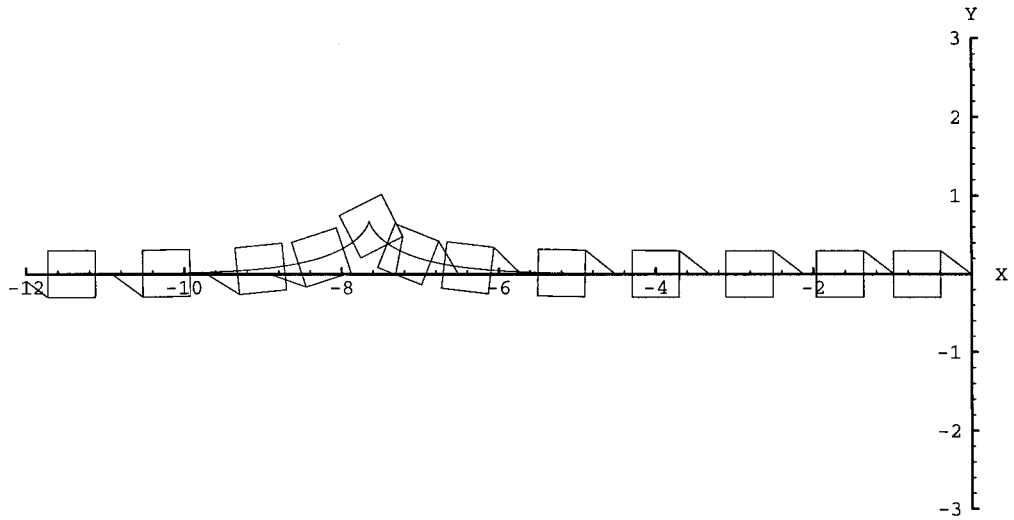

Figure 5. The trajectory of the mobile platform in Case 3 from the simulation. The mobile platform exhibits a swiveling motion.

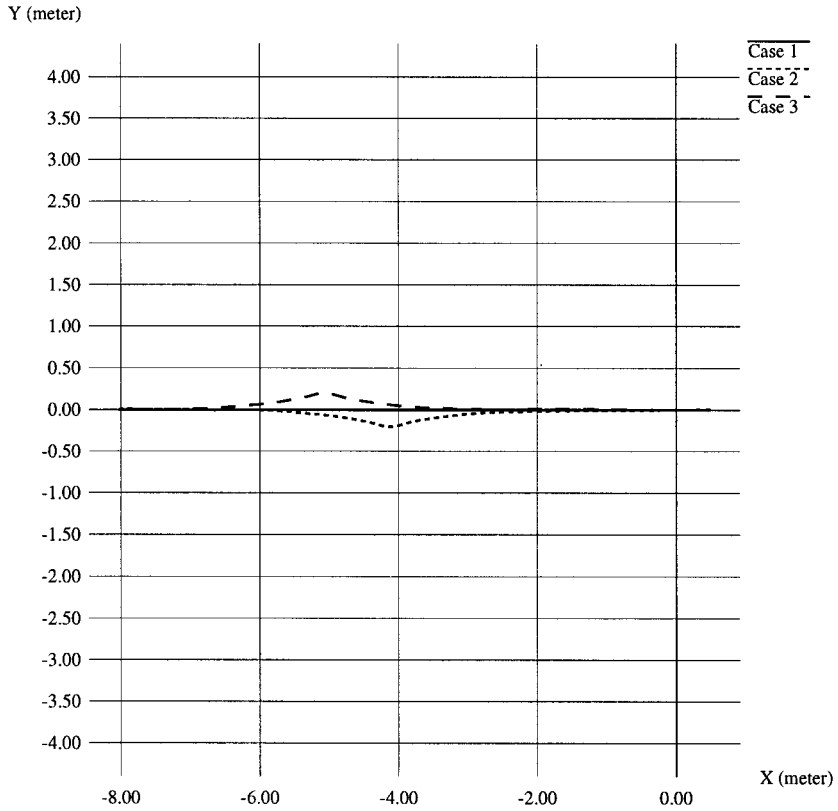

Figure 6. The actual trajectories of the reference point from the experiment.

On the other hand, if the reference point is controlled to move in the positive **X** direction, the velocity of the reference point is

$$\begin{bmatrix} \dot{y}_1 \\ \dot{y}_2 \end{bmatrix} = \begin{bmatrix} \dot{z}_2 \\ \dot{z}_4 \end{bmatrix} = \begin{bmatrix} \nu(t) \\ 0 \end{bmatrix}$$

where $\nu(t) > 0$. Using the same Liapunov function, it can be similarly shown that

$$\dot{V}(\zeta) = -\frac{\nu(t)}{L} \sin^2(c\zeta_1 - c\zeta_2)$$

along the forward internal motion. Therefore, the forward internal motion is stable.

To state the results in terms of driving experience, the internal dynamics of the vehicle are stable when driving forwards, and unstable when driving backwards (the driver still looking at a point in front of the vehicle in analogy to the look-ahead control).

5. SIMULATION AND EXPERIMENTAL RESULTS

Simulations and experiments have been conducted to verify the theoretical analysis presented in the preceding section. In particular, simulations and experiments are focused on the verification of unstable behaviors when the mobile robot is commanded to move backward. The desired trajectory for the reference point is chosen to be

$$y_1^d(t) = -V_x t \tag{38}$$

$$y_2^d(t) = 0 \tag{39}$$

where $V_x > 0$ is the desired velocity. The following parameters are used in both simulations and experiments: $L = 0.487$ m, $b = 0.171$ m, $r = 0.0228$ m, $d = 0$ m, and $c = 0.0667$.

Depending on the initial conditions of the state variable x, the following three cases are examined in simulations and experiments:

1. The initial value of x_1 and x_2 are chosen such

that the actual reference point coincides with the desired trajectory at $t = 0$, i.e.,

$$y_1(0) = y_1^d(0) = 0$$
$$y_2(0) = y_2^d(0) = 0$$

The initial values of θ_1, θ_2, η_1, and η_2 are all set to zero. Consequently, the initial heading angle is zero.

2. The initial values of θ_1 and θ_2 are chosen such that the initial heading angle $\phi(t = 0) = c(\theta_1(0) - \theta_2(0)) = 0.1$ degrees. All other initial conditions are the same as in case 1.

3. The initial conditions are the same as in case 1. However, a disturbance in the heading angle is introduced in the middle of the trajectory. In simulations, the disturbance is introduced by adding $\Delta\phi = 0.1$ degrees to the actual heading angle for two sampling intervals 3.0 s later. In experiments, the disturbance is introduced by placing a magazine in the path of the vehicle. When one of the driving wheels runs over the magazine, the heading angle is altered slightly due to different floor conditions at the two wheels.

5.1. Simulations

Simulations are conducted with the sampling rate of 100 Hz. Figure 2 shows the actual trajectory of the reference point, and Figure 3 shows that of the point P_0 for the three cases. Figure 4 depicts the trajectory of the heading angle. In all three cases, the reference point follows the desired trajectory very closely. (The three curves in Figure 2 coincide with the X-axis.) Nevertheless, the internal motions of the mobile platform corresponding to the three cases are distinctively different. In the first case, the mobile platform moves backward without changing the heading angle. In the second and third cases, while the reference point tracks the desired trajectory, the mobile platform itself exhibits a swiveling motion and changes the heading angle by 180 degrees. To clearly see the swiveling motion, the trajectory for the third case is repeated in Figure 5 in which a box and the tip of the line extended from a corner of the box represent the platform and the reference point, respectively. Therefore, these simulation results support that the internal motion of the mobile platform when the reference point moves in the negative **X** direction is unstable.

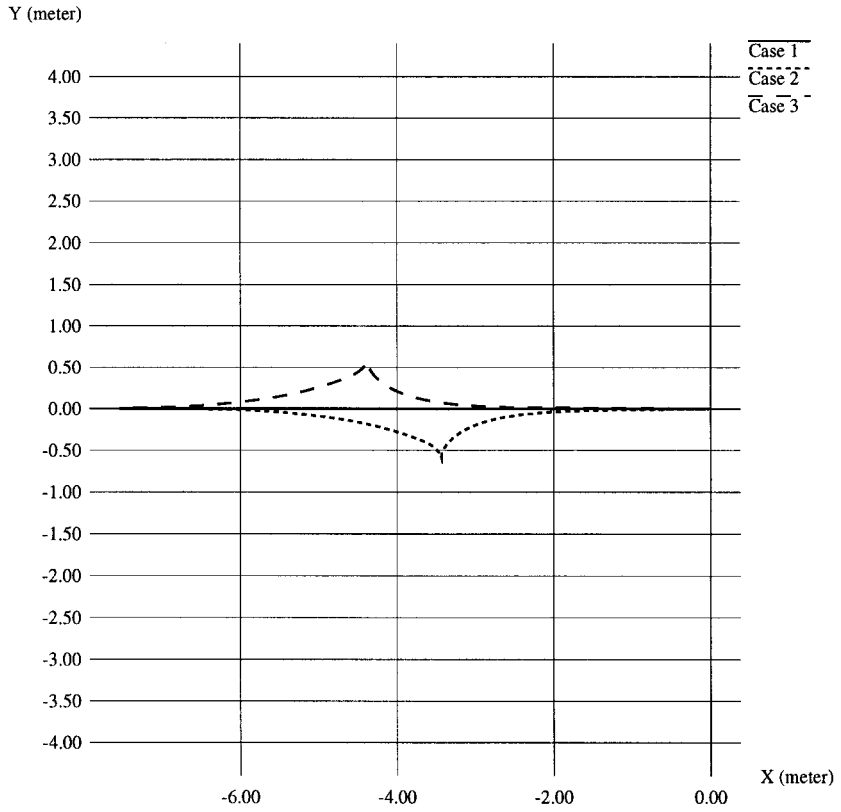

Figure 7. The trajectories of P_0 on the wheel axis from the experiment.

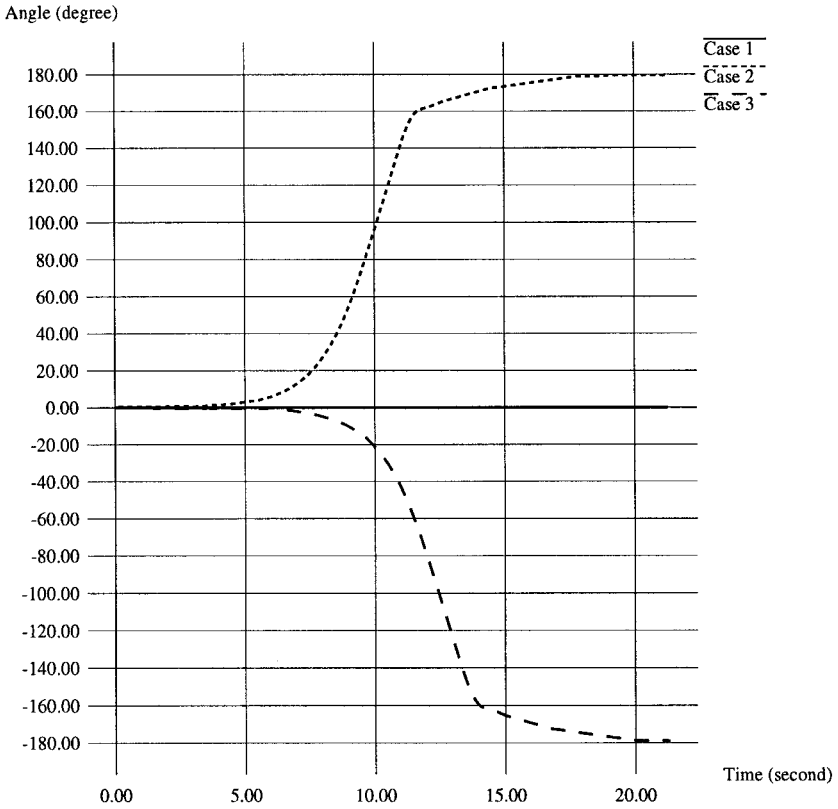

Figure 8. The heading angles of the LABMATE from the experiment.

5.2. Experiments

Experiments are conducted using a LABMATE[b] mobile platform that is controlled with the sampling rate of 9 Hz. The trajectories of the reference point and the point P_0 for the three cases are shown in Figures 6 and 7, respectively. Also the trajectory of the heading angle is shown in Figure 8. The experimental results show strong correlations with the simulation results. A minor difference appears in the trajectories of the reference point, comparing Figure 2 and Figure 6. In the experiment, the reference point has some noticeable deviations from the desired trajectory while the mobile platform is making the swiveling motion. Nevertheless, it is evident that the internal dynamics of the mobile platform are unstable when it moves backwards.

6. CONCLUSION

Stability properties of the internal dynamics of a wheeled mobile robot were investigated. Although the internal dynamics do not show up in the input-output map, they do affect the behavior of the mobile robot. In particular, when the mobile robot moves backwards, it tends to swivel itself by 180 degrees subject to small disturbances. It is important to keep this result in mind when planning trajectories of mobile robots in the same way as we plan for driving: driving backwards over a short distance is feasible, but driving backwards over a substantially long distance is not advisable (it would be easier to make a U-turn and drive forwards.)

The phenomenon of unstable mobile robot behaviors has been observed earlier. However, for the first time, stability properties of the internal dynamics are fully analyzed using the Liapunov stability theory. For a two-wheel differential-drive mobile robot under the look-ahead control, the internal dynamics are precisely described. Using a novel Liapunov function, it is shown that the internal dynamics when the mobile robot moves forward are stable, but the internal dynamics when it moves backwards are unstable. The result is confirmed by both computer simulation and physical experiment.

[b] LABMATE is a trademark of Transitions Research Corporation.

This work was supported in part by NSF grants IRI-95-96026 and CDA-95-96021, and the NPS RIP grant.

REFERENCES

1. B. d'Andrea Novel, G. Bastin, and G. Campion, ''Modelling and control of non holonomic wheeled mobile robots,'' *Proc. 1991 Int. Conf. Robotics Automat.,* Sacramento, CA, 1991, pp. 1130–1135.
2. C. Samson and K. Ait-Abderrahim, ''Feedback control of a nonholonomic wheeled cart in cartesian space,'' *Proc. 1991 Int. Conf. Robotics Automat.,* Sacramento, CA, 1991, pp. 1136–1141.
3. C. Canudas de Wit and R. Roskam, ''Path following of a 2-DOF wheeled mobile robot under path and input torque constraints,'' *Proc. 1991 Int. Conf. Robotics Automat.,* Sacramento, CA, 1991, pp. 1142–1147.
4. B. d'Andrea Novel, B. Bastin, and G. Campion, ''Dynamic feedback linearization of nonholonomic wheeled mobile robots,'' *Proc. 1992 Int. Conf. Robotics Automat.* Nice, France, 1992, pp. 2527–2532.
5. A. M. Bloch and N. H. McClamroch, ''Control of mechanical systems with classical nonholonomic constraints,'' *Proc. 28th IEEE Conf. Decision and Control,* Tampa, FL, 1989, pp. 201–205.
6. A. M. Bloch, M. Reyhanoglu, and N. H. McClamroch, ''Control and stabilization of nonholonomic dynamic systems,'' *IEEE Trans. Automatic Control,* **37**(11); 1746–1757, 1992.
7. Y. Yamamoto and X. Yun, ''Coordinating locomotion and manipulation of a mobile manipulator,'' *IEEE Trans. on Automatic Control,* **39**(6), 1326–1332, 1994.
8. C. Samson and K. Ait-Abderrahim, ''Mobile robot control part 1: Feedback control of non holonomic wheeled cart in cartesian space,'' INRIA Technical Report No. 1288, Sophia-Antipolis, France, 1990.
9. Y. Kanayama, Y. Kimura, F. Miyazaki, and T. Noguchi, ''A stable tracking control method for an autonomous mobile robot,'' *Proc. 1990 Int. Conf. Robotics Automat.,* Cincinnati, OH, 1990, pp. 384–389.
10. R. M. Rosenberg, *Analytical Dynamics of Discrete Systems,* Plenum Press, New York, 1977.
11. A. Isidori, *Nonlinear Control Systems: An Introduction,* Springer-Verlag, New York, 1985.
12. J. J. E. Slotine and W. Li, *Applied Nonlinear Control,* Prentice Hall, Inc., Englewood Cliffs, New Jersey, 1991.
13. A. De Luca, ''Zero dynamics in robotic systems,'' in *Nonlinear Synthesis,* C. I. Byrnes and A. Kurzhandsky, Eds., Birkhauser, Boston, MA, 1991, pp. 68–87.